

# Odf2-deficient mother centrioles lack distal/subdistal appendages and the ability to generate primary cilia

Hiroaki Ishikawa<sup>1,2</sup>, Akiharu Kubo<sup>1,2</sup>, Shoichiro Tsukita<sup>1,2</sup> and Sachiko Tsukita<sup>1-4</sup>

**Outer dense fibre 2 (Odf2; also known as cenexin) was initially identified as a main component of the sperm tail cytoskeleton, but was later shown to be a general scaffold protein that is specifically localized at the distal/subdistal appendages of mother centrioles<sup>1,2</sup>. Here we show that Odf2 expression is suppressed in mouse F9 cells when both alleles of *Odf2* genes are deleted. Unexpectedly, the cell cycle of *Odf2*<sup>-/-</sup> cells does not seem to be affected. Immunofluorescence and ultrathin-section electron microscopy reveals that in *Odf2*<sup>-/-</sup> cells, distal/subdistal appendages disappear from mother centrioles, making it difficult to distinguish mother from daughter centrioles. In *Odf2*<sup>-/-</sup> cells, however, the formation of primary cilia is completely suppressed, although ~25% of wild-type F9 cells are ciliated under the steady-state cell cycle. The loss of primary cilia in *Odf2*<sup>-/-</sup> F9 cells can be rescued by exogenous Odf2 expression. These findings indicate that Odf2 is indispensable for the formation of distal/subdistal appendages and the generation of primary cilia, but not for other cell-cycle-related centriolar functions.**

The centrosomes serve as the organizing centre for the microtubule network in most animal cells, integrating and orchestrating microtubule-related cellular events such as the cell cycle, cell division, cell polarization and cell motility<sup>3-5</sup>. The centrosome consists of two centrioles that are surrounded by electron-dense pericentriolar material, which anchors the microtubules. The centrioles are each composed of nine triplets of short microtubules, arranged to form the wall of the cylinder. The centrioles need to be duplicated in the cell cycle in a semi-conservative way to provide each daughter cell with a complete pair of centrioles<sup>6</sup>. A cell has two centrioles in G1/G0 phase<sup>6,7</sup>. The mother centriole was generated at least two cell cycles ago, and constitutes a major microtubule organizing centre (MTOC). Only the mature mother centriole retains the ability to nucleate a primary cilium at its distal end<sup>8,9</sup>. Primary cilia contain 9 + 0 axonemes consisting of nine outer doublet microtubules, but lacking the central pair of microtubules, and are formed in many G1/G0 cells in culture as well as in most cell types within the body<sup>10</sup>. The daughter

centriole is produced in the previous cell cycle and is immature in a variety of its structural and functional features. When the daughter centriole begins to mature in S phase, each of the mother and daughter centrioles nucleates one procentriole at its proximal end. These procentrioles subsequently elongate to full-length centrioles, usually in S or G2 phase, resulting in two pairs of mother and daughter centrioles<sup>7</sup>.

The mother centriole is ultrastructurally distinguished from the daughter centriole by its fibrous distal and subdistal appendages<sup>11</sup>; in this study, we simply call them appendages. Several components — Odf2 (ref. 2; the cenexin antigen<sup>1</sup>), ninein<sup>12</sup>,  $\epsilon$ -tubulin<sup>13</sup>, centriolin<sup>14</sup> and CEP110 (ref. 15) — are localized in these appendages. However, most of them, except for Odf2, are not restricted to the appendages in centrioles. In addition to the appendages, ninein and CEP110 are concentrated at the proximal regions of both mother and daughter centrioles<sup>12,15</sup>. Recently, silencing of ninein,  $\epsilon$ -tubulin, centriolin and CEP110 by RNA-mediated interference (RNAi) or antibody injection has been reported to affect the cell-cycle progression and/or the MTOC activity<sup>13-16</sup>. This suggests that appendage proteins of mother centrioles are involved in the fundamental roles of centrioles such as centriolar duplication and nucleation of microtubules.

Odf2 is unique in its exclusive localization at the appendages of the mother centrioles. Therefore, to evaluate the physiological functions of the appendages more specifically, we attempted to examine the effects of Odf2 silencing on the centriolar functions. We knocked out both alleles of *Odf2* genes to suppress the expression of Odf2 completely and stably. The mutant allele of *Odf2* was generated in F9 cells by homologous recombination, and two phenotypically identical clones of F9 cells (*Odf2*<sup>-/-</sup> cells) homozygous for a targeted mutation in the *Odf2* locus were obtained (see Supplementary Information, Fig. S1). Disruption of *Odf2* was confirmed by Southern blotting. Immunoblotting with anti-Odf2 polyclonal antibody clearly detected a band with a relative molecular mass of ~90,000 ( $M_r$  90K) in *Odf2*<sup>+/+</sup> and *Odf2*<sup>+/-</sup> cells, but not in *Odf2*<sup>-/-</sup> cells.

When cells were cultured on a coverslip, phase contrast microscopy identified no difference in appearance between *Odf2*<sup>+/+</sup> and *Odf2*<sup>-/-</sup> cells (data not shown). *Odf2*<sup>-/-</sup> cells appeared to proliferate normally, which is distinct from cells in which the expression of other components of the appendage was suppressed. Simple cell counting revealed that *Odf2*<sup>-/-</sup> cells

<sup>1</sup>Department of Cell Biology, Faculty of Medicine, Kyoto University, Sakyo-ku, Kyoto 606-8501, Japan. <sup>2</sup>Solution Oriented Research for Science and Technology, Japan Science and Technology Corporation, Sakyo-ku, Kyoto 606-8501, Japan. <sup>3</sup>School of Health Sciences, Faculty of Medicine, Kyoto University, Sakyo-ku, Kyoto 606-8507, Japan.

<sup>4</sup>Correspondence should be addressed to Sa.T. (e-mail: atsukita@mfour.med.kyoto-u.ac.jp)

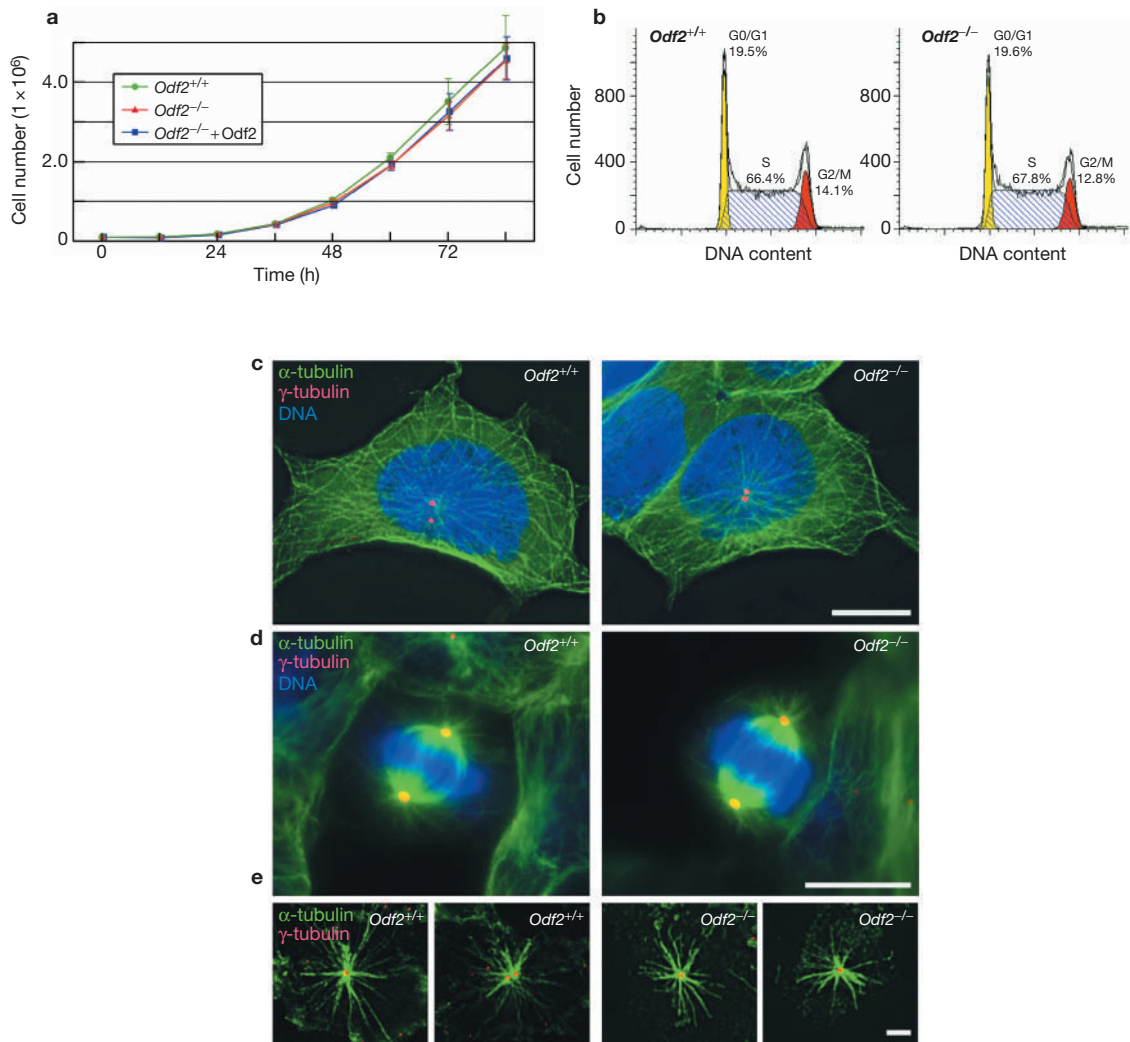


**Figure 1** Cell growth, cell cycle and microtubule organization of *Odf2*<sup>+/+</sup> and *Odf2*<sup>-/-</sup> F9 cells. **(a)** Cell growth curve of the following F9 cells: *Odf2*<sup>+/+</sup> (green), *Odf2*<sup>-/-</sup> (red) and *Odf2*<sup>-/-</sup> cells expressing exogenous *Odf2* (+ *Odf2*; blue). Cells ( $1 \times 10^5$  cells) were cultured on 6-well plates. Every 12 h, cells were dissociated into single cells by treatment with 0.25% trypsin/1 mM EDTA at 37 °C for 5 min. Cell growth was measured by making duplicate counts of these cells with a haemocytometer. Note that these three types of cell grew with the same time course. Error bars represent s.d. calculated from four independent experiments. **(b)** Proportion of *Odf2*<sup>+/+</sup> (left graph) and *Odf2*<sup>-/-</sup> (right graph) F9 cells in the G0/G1, G2/M and S phase. The proportion was estimated by triplicate measurements using FACS analysis and the ModFit cell-cycle analysis program. No significant difference was discerned between *Odf2*<sup>+/+</sup> and

*Odf2*<sup>-/-</sup> F9 cells. **(c, d)** Organization of microtubules in *Odf2*<sup>+/+</sup> and *Odf2*<sup>-/-</sup> F9 cells. Cells were triple-stained with anti- $\alpha$ -tubulin monoclonal antibody (green), anti- $\gamma$ -tubulin polyclonal antibody (red) and 4,6-diamidino-2-phenylindole (DAPI; blue) at the interphase **(c)** and mitotic phase **(d)**. The *Odf2* deficiency did not affect microtubule organization throughout the cell cycle. Scale bar, 10  $\mu$ m. **(e)** MTOC activities of centrosomes in *Odf2*<sup>+/+</sup> and *Odf2*<sup>-/-</sup> F9 cells. Cells were incubated in a medium containing 1  $\mu$ M nocodazole for 1 h to depolymerize microtubules, washed/incubated with a fresh medium for 2 min to re-polymerize the microtubules, and then processed for immunofluorescence microscopy with anti- $\alpha$ -tubulin monoclonal antibody (green) and anti- $\gamma$ -tubulin polyclonal antibody (red). *Odf2*<sup>+/+</sup> and *Odf2*<sup>-/-</sup> centrosomes appeared to nucleate microtubules to the same extent. Scale bar, 2  $\mu$ m.

had the same growth curve as *Odf2*<sup>+/+</sup> cells (Fig. 1a), and cell-cycle analysis showed no changes in cell-cycle progression (Fig. 1b). When *Odf2*<sup>-/-</sup> cells were double-stained with  $\alpha$ - and  $\gamma$ -tubulin antibodies, the organization of microtubule networks or the localization/behaviour of centrosomes did not seem to be affected by the *Odf2* deficiency in F9 cells, not only at interphase but also in mitosis (Fig. 1c, d). We then compared the MTOC activity of centrosomes in *Odf2*<sup>+/+</sup> and *Odf2*<sup>-/-</sup> cells (Fig. 1e). Cells were incubated in a medium containing 1  $\mu$ M nocodazole for 1 h to depolymerize microtubules, then washed with fresh medium, and incubated in fresh medium to re-polymerize the microtubules. They were then processed for immunofluorescence microscopy with anti- $\alpha$ - and anti- $\gamma$ -tubulin antibodies. Judging from the size and microtubule density of reconstructed

aster-like structures, we concluded that there was no significant difference in the MTOC activity between *Odf2*<sup>+/+</sup> and *Odf2*<sup>-/-</sup> centrosomes.

We then examined the centrosomes in *Odf2*<sup>-/-</sup> cells and investigated the appendages and their components. First, paired centrosomes of *Odf2*<sup>+/+</sup> and *Odf2*<sup>-/-</sup> cells at G1 phase were triple-stained with antibodies specific for *Odf2*, ninein and  $\gamma$ -tubulin (Fig. 2a, b). Three ninein-positive dots on mother  $\gamma$ -tubulin-positive centrosomes and one ninein-positive dot on daughter  $\gamma$ -tubulin-positive centrosomes were identified in *Odf2*<sup>+/+</sup> cells<sup>12,15</sup>. On both centrosomes, ninein was concentrated as a dot on their proximal ends. On only the mother centrosome, an additional two ninein-positive dots were detected at the appendages (see schematic drawings in Fig. 2b). In sharp contrast, *Odf2* was detected only on the mother

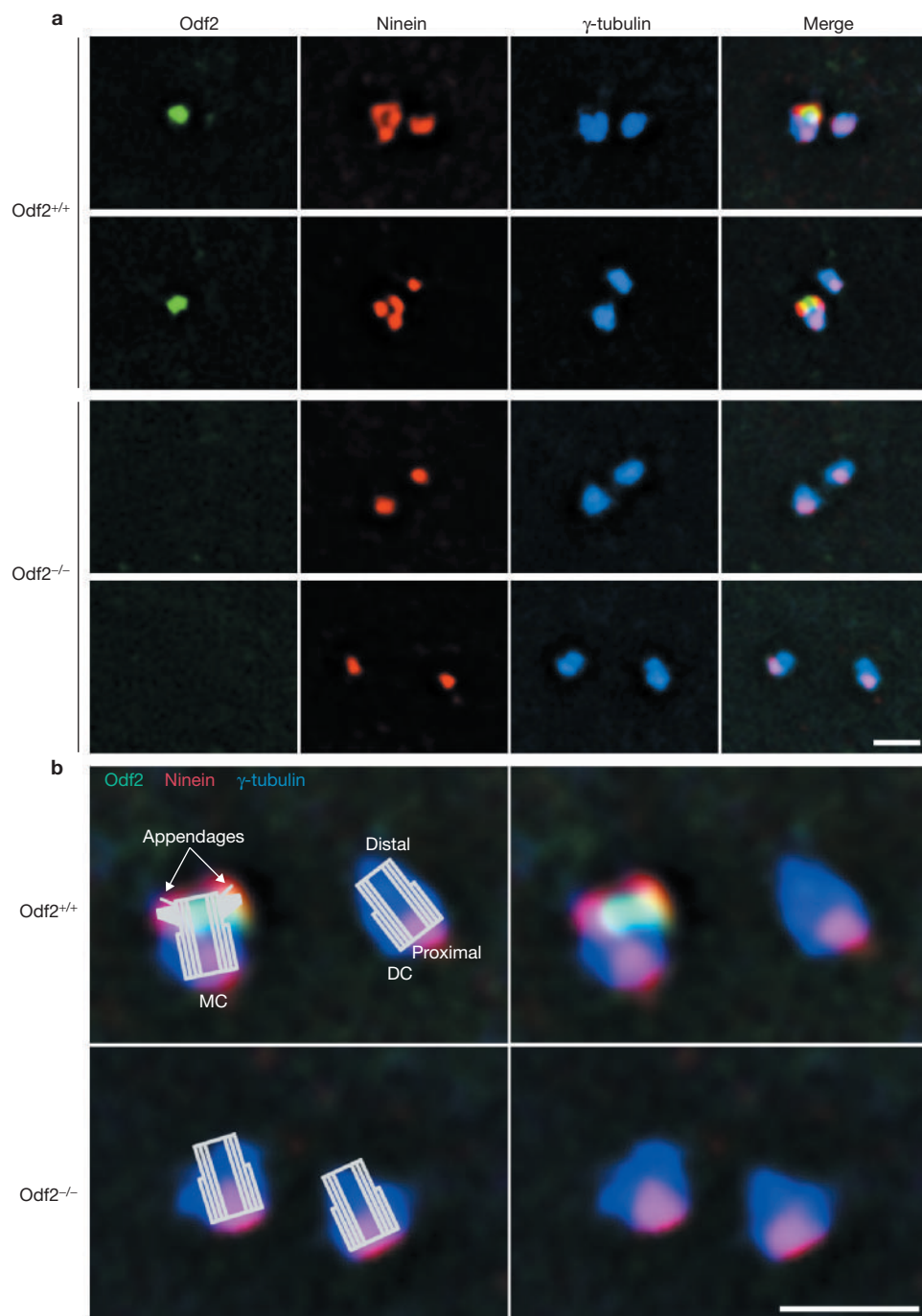


**Figure 2** The appendages of the mother centrioles in *Odf2*<sup>+/+</sup> and *Odf2*<sup>-/-</sup> F9 cells. (a) Triple immunofluorescence labelling of paired centrioles for Odf2, ninein and  $\gamma$ -tubulin. In *Odf2*<sup>+/+</sup> cells, both mother and daughter centrioles were positive for  $\gamma$ -tubulin (blue). As previously reported, Odf2 was highly enriched in the distal end of mother centrioles (green)<sup>2</sup>, whereas three ninein-positive dots on mother and one ninein-positive dot on daughter centrioles were detected (red)<sup>12,15</sup>. In *Odf2*<sup>-/-</sup> cells, the Odf2 signal was undetectable,

but the staining pattern for  $\gamma$ -tubulin did not appear to be affected (blue). Interestingly, two of the three ninein-positive dots on the mother centriole disappeared, leaving one dot on the proximal end of mother and daughter centrioles (red). Scale bar, 1  $\mu$ m. (b) Possible spatial relationship between the Odf2, ninein and  $\gamma$ -tubulin signals and the ultrastructure of centrioles. This schematic was drawn on the basis of previous reports<sup>5,11</sup>. MC, mother centriole; DC, daughter centriole. Scale bar, 1  $\mu$ m.

centriole, and was concentrated at its distal end as one dot. On the basis of previous observations, these Odf2-positive dots could also represent the appendages<sup>2</sup>, but the triple-staining clearly indicated that along appendages Odf2 concentrated much closer than ninein to the centriolar triplet cylinder. In paired centrioles of *Odf2*<sup>-/-</sup> cells, Odf2 was undetectable by immunofluorescence staining, and Odf2 deficiency did

not affect the appearance of  $\gamma$ -tubulin-positive centrioles *per se* (Fig. 2a, b). Interestingly, both paired centrioles bore only single ninein-positive dots on their proximal ends. In *Odf2*<sup>-/-</sup> centrioles, ninein on the appendages of the mother centriole completely disappeared, leaving a single ninein-positive dot on its proximal end (see schematic drawings in Fig. 2b), suggesting an Odf2-independent localization of ninein on its

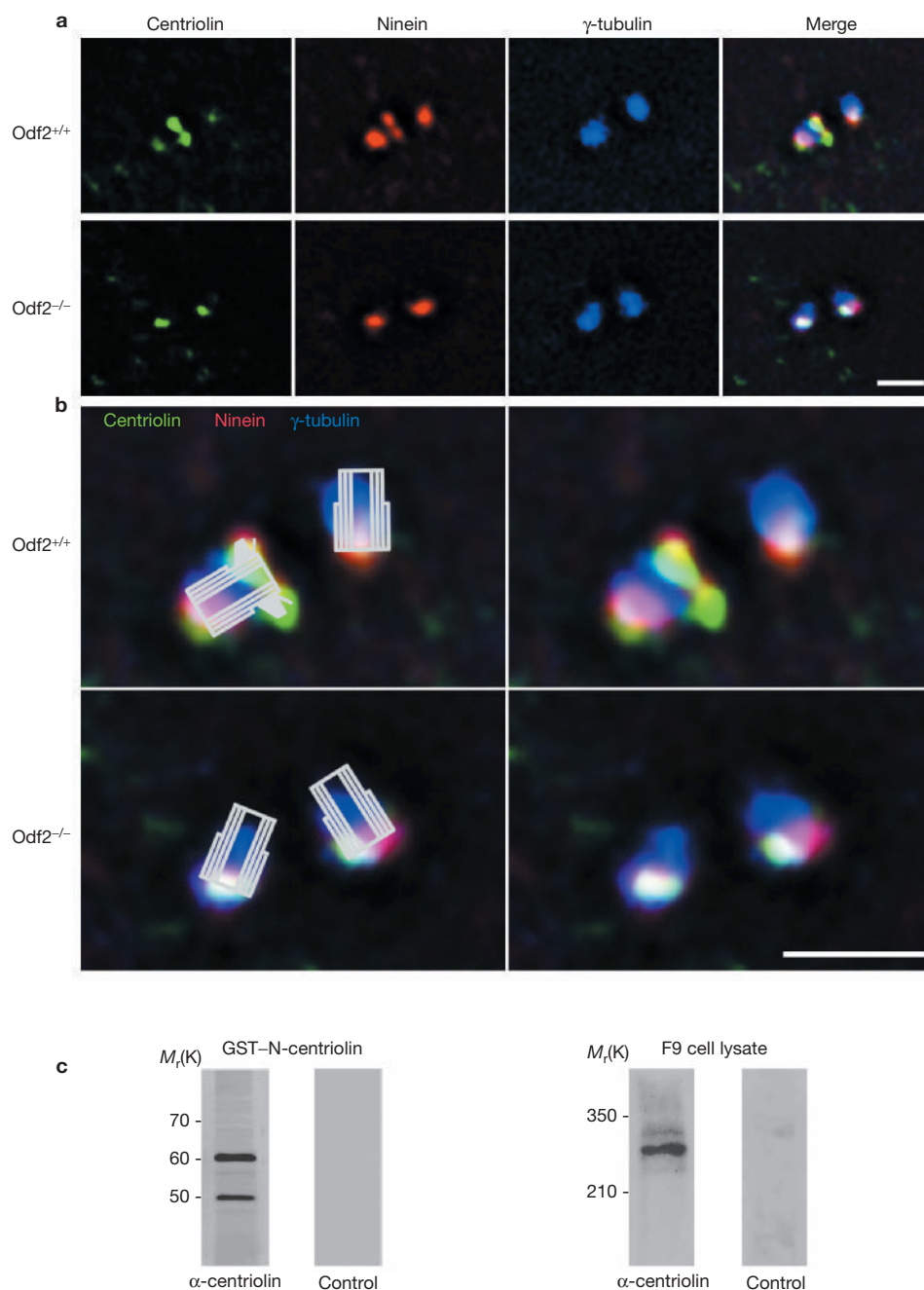


**Figure 3** Localization of centriolin in *Odf2*<sup>+/+</sup> and *Odf2*<sup>-/-</sup> F9 cells. **(a)** Triple immunofluorescence labelling of paired centrioles for centriolin (green), ninein (red) and γ-tubulin (blue). In *Odf2*<sup>+/+</sup> cells, both mother and daughter centrioles were positive for γ-tubulin. As previously reported<sup>12,15</sup>, three centriolin- and ninein-double-positive dots on mother and one double-positive dot on daughter centrioles were detected. In *Odf2*<sup>-/-</sup> cells, two of the three centriolin- and ninein-positive dots on the mother centriole disappeared, leaving

proximal end. Furthermore, centriolin, another component of appendages<sup>14</sup>, showed a very similar distribution to that of ninein on *Odf2*<sup>+/+</sup> centrioles, and behaved very similarly to ninein on *Odf2*<sup>-/-</sup> centrioles (Fig. 3). These findings indicate that *Odf2* is necessary for localization of ninein (and also centriolin) to the appendages of the mother centriole, or for the formation of the appendages.

We next examined by serial, ultrathin-section electron microscopy whether the appendage itself disappears from mother centrioles in

one centriolin- and ninein-positive dot on the proximal end of mother and daughter centrioles. Scale bar, 1 μm. **(b)** Possible spatial relationship between the centriolin, ninein and γ-tubulin signals, and the ultrastructure of centrioles. This schematic was drawn on the basis of previous reports<sup>5,11</sup>. Scale bar, 1 μm. **(c)** Immunoblotting of GST-N-centriolin fusion protein and F9 cell lysate with anti-centriolin antibody (α-centriolin). Anti-centriolin polyclonal antibody recognized specifically the fusion protein and the endogenous centriolin.

*Odf2*<sup>-/-</sup> cells. *Odf2*<sup>+/+</sup> and *Odf2*<sup>-/-</sup> cells were cultured on Transwell filters and serial ultrathin sections were obtained (Fig. 4). In *Odf2*<sup>+/+</sup> cells that bore only one pair of centrioles at G1/G0 phase, typical appendages were reproducibly identified at the distal end of one of the paired centrioles. Numerous microtubules appeared to radiate out into the cytoplasm from the distal regions of these 'mother' centrioles. In contrast, in *Odf2*<sup>-/-</sup> F9 cells the appendages were never observed to be associated with centrioles throughout serial ultrathin sections. The loss of



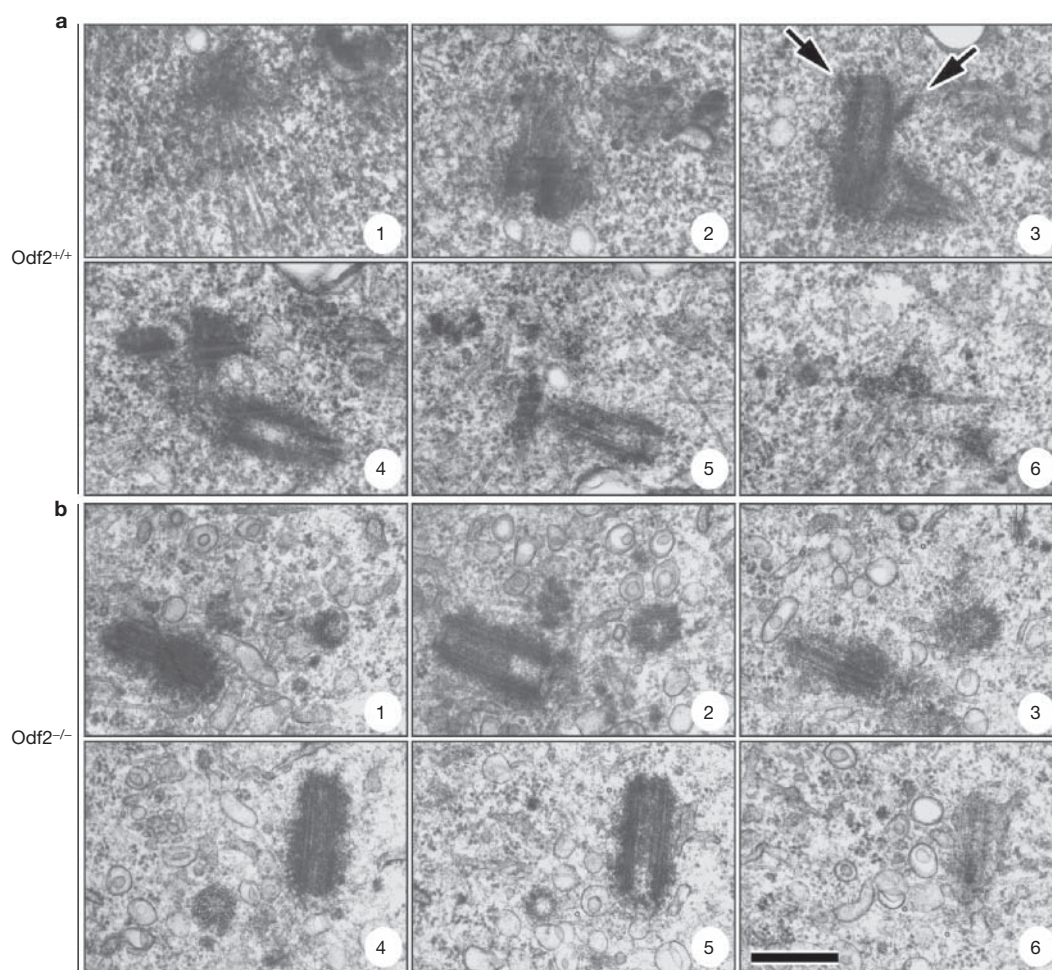


**Figure 4** Serial ultrathin-section electron micrographs of paired centrosomes in *Odf2*<sup>+/+</sup> and *Odf2*<sup>-/-</sup> F9 cells. (**a**, **b**) Series **a** and **b** identify six levels including the whole paired centrosomes. Appendages

(arrows) are detected in the distal region of the mother centriole in *Odf2*<sup>+/+</sup> F9 cells, but are not detected in either centriole in *Odf2*<sup>-/-</sup> F9 cells. Scale bar, 400 nm.

appendages made it difficult to distinguish mother from daughter centrioles, morphologically, but microtubules were still observed around centrioles. Taking into consideration that ninein (and centriolin) disappeared from the distal ends of *Odf2*<sup>-/-</sup> centrioles, these findings indicate that *Odf2* has a central and specific role in the formation of appendages on mother centrioles. Furthermore, it is safe to say that these appendages are not directly involved in centriolar duplication or in the MTOC activity of centrosomes (see Fig. 1).

Thus, the next important question is what the physiological function of the appendages on mother centrioles is. Centrioles are known to be recruited to plasma membranes at G1/G0 phase to generate a primary cilium<sup>10</sup>. Previous electron microscopic observations have reported that during primary ciliogenesis, the mother centriole — which functions as a basal body of the primary cilium — was attached to the plasma membranes at its distal end, and that the appendages appeared to be involved in this attachment<sup>17</sup>. Therefore, we first examined whether primary cilia could be observed in *Odf2*<sup>+/+</sup> F9 cells. To visualize primary cilia, *Odf2*<sup>+/+</sup> cells were immunofluorescently stained with monoclonal antibody against acetylated tubulin, which is highly concentrated at primary cilia<sup>18</sup>. As shown in Fig. 5a, primary cilia were clearly detected on the surface of ~25% *Odf2*<sup>+/+</sup> cells (552 cells were examined; see

Supplementary Information, Fig. S2). Paired centrioles were also positive for acetylated tubulin, and an acetylated tubulin-positive elongated primary cilium originated from one of the centrioles that was positive for *Odf2* (Fig. 5b). Close inspection showed that the primary cilium appeared to originate from the *Odf2*-positive end; that is, the distal end of the mother centriole. In contrast, no primary cilia were observed on the cell surface of *Odf2*<sup>-/-</sup> cells (Fig. 5a) (592 cells were examined; see Supplementary Information, Fig. S2). Furthermore, when *Odf2* was exogenously expressed in *Odf2*<sup>-/-</sup> cells by the  $\beta$ -actin-driven expression vector system, primary cilia were generated again on the cell surface of ~12% cells (Fig. 5a) (366 cells were examined; see Supplementary Information, Fig. S2). These findings clearly indicate that *Odf2* is indispensable for the formation of primary cilia.

In recent years, primary cilia have attracted increasing interest. It is suggested that left–right asymmetry is established by an entirely ciliary mechanism at the initial phase of mouse embryogenesis: motile, left–right dynein-containing primary cilia generate nodal flow, and nonmotile polycystin-2-containing primary cilia sense nodal flow, initiating an asymmetric calcium signal at the left border of the node<sup>19</sup>. Recent findings on the molecular pathogenesis of hereditary polycystic kidney disease (PKD) were characterized by the formation of multiple epithelial cysts

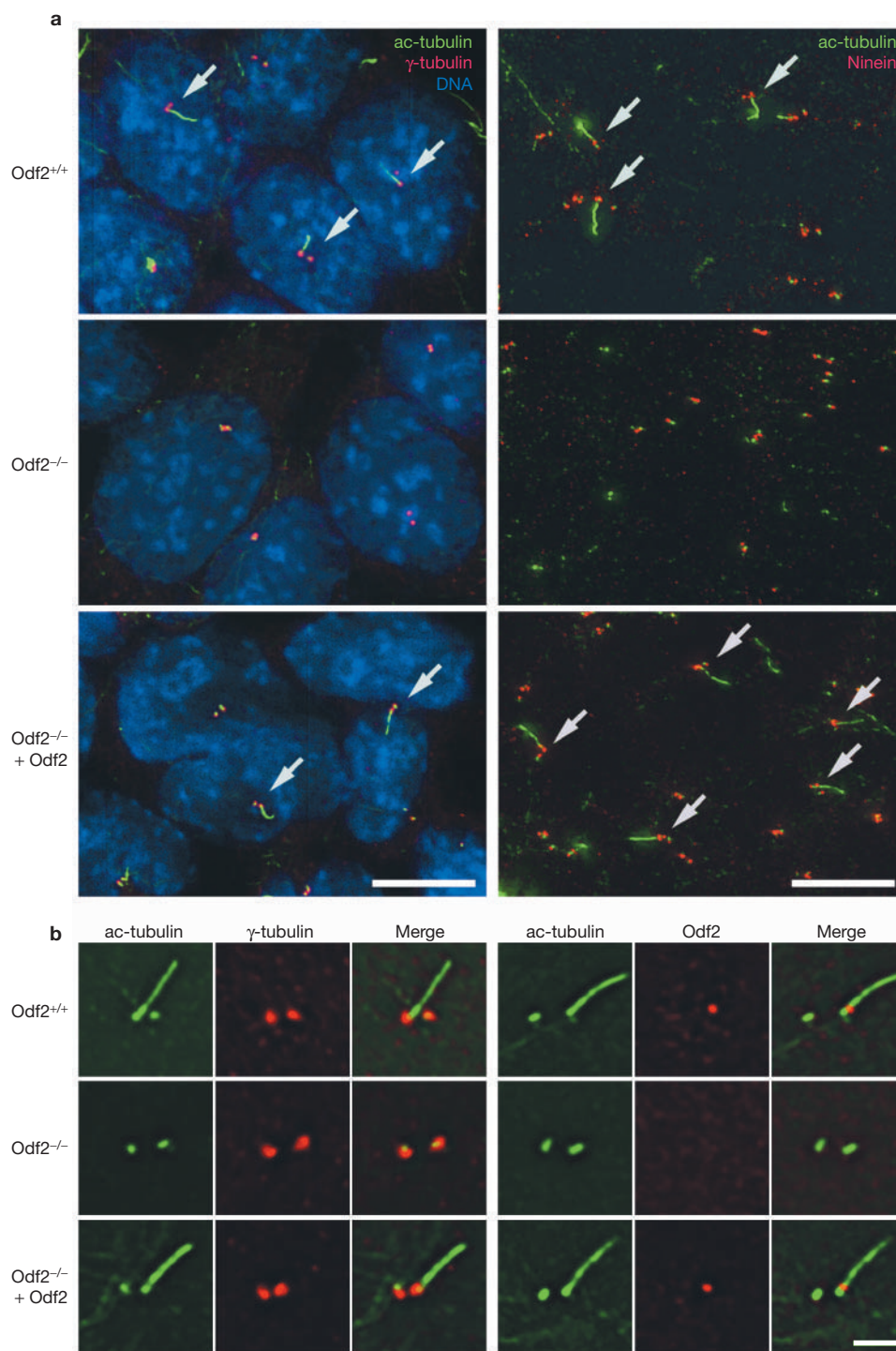


**Figure 5** Loss of primary cilia in *Odf2*<sup>-/-</sup> F9 cells. (a) Double immunostaining of the following F9 cells: *Odf2*<sup>+/+</sup>, *Odf2*<sup>-/-</sup>, and *Odf2*<sup>-/-</sup> expressing exogenous Odf2 (*Odf2*<sup>-/-</sup> + Odf2). Cells were stained with anti-acetylated tubulin (ac-tubulin) monoclonal antibody (green), anti- $\gamma$ -tubulin polyclonal antibody (red) or DAPI (blue) (left panels), or with anti-acetylated tubulin monoclonal antibody (green) or anti-ninein polyclonal antibody (red) (right panels). Acetylated-tubulin-positive-primary cilia (arrows) were detected on the cell surface of ~25% of *Odf2*<sup>+/+</sup> F9 cells. Under the same culture conditions, no primary cilia were observed on the surface of any *Odf2*<sup>-/-</sup> F9 cells. The loss of primary cilia in *Odf2*<sup>-/-</sup> F9 cells

was rescued by exogenous expression of Odf2 (arrows; *Odf2*<sup>-/-</sup> + Odf2). Scale bar, 10  $\mu$ m. (b) High-power images of centrioles. Cells were double-stained with anti-acetylated tubulin monoclonal antibody (green) or anti- $\gamma$ -tubulin polyclonal antibody (red) (left panel), or with anti-acetylated tubulin monoclonal antibody (green) or anti-Odf2 polyclonal antibody (red) (right panel). When Odf2 was detected in mother centrioles (*Odf2*<sup>+/+</sup> and *Odf2*<sup>-/-</sup> + Odf2), acetylated tubulin-positive primary cilia were generated from the distal end of the mother centriole, where Odf2 was concentrated as a dot. *Odf2*<sup>-/-</sup> centrioles lack primary cilia without exception. Scale bar, 2  $\mu$ m.



in the kidney, and have made a further impact on the field of primary cilia<sup>20</sup>. Mutations in polycystin-1 or polycystin-2 accounted for all cases of autosomal-dominant PKD in the human<sup>21,22</sup>, and mutations in polaris and cystin caused autosomal-recessive PKD in the mouse<sup>23,24</sup>. Notably, these gene products were all concentrated at primary cilia of epithelial cells in the normal kidney<sup>25</sup>. The molecular mechanisms underlying how dysfunctions of these proteins cause PKD remain unclear. However, taking into consideration that forced bending of primary cilia increases the intracellular  $\text{Ca}^{2+}$  ion in cultured epithelial cells<sup>26</sup>, primary cilia are now believed to be physiologically more important in epithelial proliferation, polarization and tubulogenesis than was previously expected<sup>27</sup>.

Primary cilia are formed in most eukaryotic cells, but our knowledge of factors that determine their assembly and disassembly is still fragmentary. In recent years, the molecular machinery involved in transporting various materials towards the distal tips of cilia — that is, intraflagellar transport (IFT) particles — has been well characterized as being composed of 15–20 proteins organized into two large complexes, A and B<sup>28</sup>. The deficiency of several IFT particle-related components such as kinesin II<sup>29</sup>, polaris<sup>23</sup> and pericentrin<sup>30</sup>, was shown to result in defects in the formation of primary cilia. The first step for formation of primary cilia is the targeting of mother centrioles to plasma membranes, but this is not reported to be a simple step. When the mother centriole comes close to plasma membranes, a peculiar membranous vesicle emerges to associate with the distal end of the triplet cylinder as well as the appendages. Ciliary microtubules then begin to elongate from the distal end. Although the association between the vesicle and the appendages appears to be maintained during this elongation process, the vesicle is deformed into a cup shape, and finally fused with plasma membranes to generate primary cilia that topologically protrude out from the cell surface. The electron microscopic observation of this process strongly suggests that appendages have an important role in the association of mother centrioles with plasma membranes<sup>17</sup>. In good agreement with this, in this study we found that in *Odf2*<sup>-/-</sup> F9 cells, appendages disappeared from mother centrioles and no primary cilia were generated. The question naturally arose as to whether in *Odf2*<sup>-/-</sup> F9 cells the docking of the mother centriole to plasma membranes was itself affected. It was difficult to conclusively address this question by ultrathin-section microscopy, but in our examination of *Odf2*<sup>+/+</sup> and *Odf2*<sup>-/-</sup> centrioles (47 and 43 cells, respectively), 11 and 0 centrioles, respectively, were attached to plasma membranes. Furthermore, when *Odf2*<sup>+/+</sup> and *Odf2*<sup>-/-</sup> F9 cells (200 for each) were double-stained for  $\gamma$ -tubulin and ERM proteins — the respective markers for centrosomes and dorsal plasma membranes — to roughly estimate the distance between centrosomes and plasma membranes by sectioning immunofluorescence microscopy, ~40% and ~10%, respectively, of the centrosomes were located within 0.8  $\mu\text{m}$  of the dorsal plasma membranes. Thus, these findings favoured the notion that *Odf2* deficiency affects the docking of centrioles to membranes, although the detailed molecular basis for this awaits future studies.

This study provides a clue for developing a new method to specifically evaluate the physiological relevance of the generation of primary cilia *in situ*. As mentioned above, distinct from other components of centrosomes, *Odf2* seems to be involved specifically in the generation of primary cilia but not in other centrosomal functions. Therefore, it would be possible to suppress primary cilia formation in a tissue-specific manner without affecting other cellular events if the *Odf2* gene were conditionally knocked out in mice. Studies are currently being conducted along this line in our laboratory. □

## METHODS

**Cells and antibodies.** Mouse F9 embryonic carcinoma cells were cultured in Dulbecco's modified Eagle's medium (DME) containing 10% heat-inactivated fetal calf serum (FCS). The cDNA encoding amino acids 41–266 of mouse *Odf2*, or 953–1228 of mouse ninein, or 1–261 of mouse centriolin (N-centriolin) was subcloned into pGEX-4T-1 (Amersham Biosciences, Piscataway, NJ), and their glutathione *S*-transferase (GST) fusion proteins were expressed in *Escherichia coli*. They were then purified by glutathione Sepharose 4B columns (Amersham Biosciences), and used as antigens for antibody production in rabbits or rats. These polyclonal antibodies were affinity-purified on polyvinylidene fluoride (PVDF) membranes with the corresponding fusion proteins. Rat anti-chicken *Odf2* monoclonal antibody was characterized previously<sup>2</sup>. Mouse anti- $\alpha$ -tubulin monoclonal antibody (DM1A), mouse anti- $\gamma$ -tubulin monoclonal antibody (GTU-88), rabbit anti- $\gamma$ -tubulin polyclonal antibody and mouse anti-acetylated-tubulin monoclonal antibody (6-11B-1) were purchased from Sigma (St Louis, MO).

**Generation of *Odf2*-deficient F9 cells.** A  $\lambda$  phage 129/Sv mouse genomic library was screened using a mouse *Odf2* cDNA fragment as a probe. The targeting vector was constructed by standard recombinant DNA techniques. A 1.2-kilobase (kb) *KpnI/KpnI* fragment containing exons 5–6 and a 5.6-kb *XhoI/SalI* fragment (with the *SalI* site derived from the vector polylinker) containing intron 10 were ligated to a targeting vector cassette. This cassette consisted of a 5' donor *engrailed-2* (*En-2*) intron containing the splice acceptor site, an internal ribosome entry site (IRES), a  $\beta$ -galactosidase/neomycin-resistance fusion gene ( $\beta$ -geo) flanked by loxP sites, and a 3' simian virus 40 polyadenylation site. The gene targeting was performed twice to delete both alleles of the *Odf2* gene as follows. The targeting vector was linearized by *NotI* digestion, and F9 cells were electroporated with 20  $\mu\text{g}$  of linearized targeting vector DNA using a Bio-Rad (Hercules, CA) Gene Pulser at 0.4 V and 25  $\mu\text{F}$ . Cells were plated on gelatin-coated culture dishes in DME medium supplemented with 10% FCS for 24 h, and were then selected by adding G418 at a final concentration of 400  $\mu\text{g ml}^{-1}$ . At day 10 of culture, G418-resistant colonies were removed and screened by Southern blotting of *EcoRI*-digested DNA with the 5' external probe. Correctly targeted clones were transiently transfected with a Cre recombinase gene to remove *En-2*, IRES and  $\beta$ -geo genes from the first targeted allele. These *Odf2*<sup>+/-</sup> cells, which were now sensitive to G418, were used for the second electroporation with the same targeting vector. Colonies resistant to G418 were screened by Southern blotting of *EcoRI*-digested DNA with the 5' external probe and correctly targeted clones; that is, *Odf2*-deficient clones were established.

**Immunofluorescence microscopy.** Cells that were cultured on gelatin-coated (0.2%) coverslips or filters were fixed with methanol for 10 min at  $-20^{\circ}\text{C}$ , washed three times with phosphate-buffered saline (PBS), and treated with 0.5% Triton X-100 in PBS for 15 min. After washing with PBS, cells were soaked in 1% bovine serum albumin (BSA), then soaked in PBS for 10 min at room temperature, and incubated with primary antibodies for 1 h in a moist chamber. Cells were then washed with PBS and incubated with Alexa Fluor 488-, 594- and 647-conjugated secondary antibodies (Molecular Probes, Eugene, OR) for 30 min. Samples were then washed with PBS, mounted in 95% glycerol-PBS containing 0.1% paraperylene diamine and 1% n-propylgalate, and then observed using a DeltaVision microscope (Applied Precision, Issaquah, WA) equipped with an Olympus IX70 microscope (Olympus, Tokyo, Japan) and a cooled charge-coupled device (CCD) system. Some images were obtained with 0.2- $\mu\text{m}$  intervals in *z*-section, deconvolved and integrated with DeltaVision software (Applied Precision).

**Electron microscopy.** Cells that were cultured on filters were fixed with 2% glutaraldehyde in PEM80 buffer (80 mM PIPES, pH 6.8; 1 mM EGTA; and 1 mM  $\text{MgCl}_2$ ) containing 1 mM GTP for 10 min at  $37^{\circ}\text{C}$  and washed with 0.1 M phosphate buffer (pH 7.2). This was followed by incubation with 1.5% glutaraldehyde and 0.5% tannic acid in 0.1 M phosphate buffer for 15 min at room temperature. Samples were then processed for ultrathin-section electron microscopy as described previously<sup>2</sup>, and examined under an electron microscope (JEM 1010; JEOL, Tokyo, Japan) at an accelerating voltage of 100 kV.

**Fluorescence-activated cell sorter (FACS) analysis.** Cells were collected by trypsin digestion, washed three times with cold PBS, and fixed in ice-cold ethanol for at least 48 h. Subsequently, cells were incubated with 0.1 mg  $\text{ml}^{-1}$  RNase A, 50  $\mu\text{g ml}^{-1}$  propidium iodide, 0.1% NP-40 and 0.1% trisodium citrate for 20 min at

4 °C. For each cell population, 30,000 cells were analysed by FACS (FACSCalibur, Becton-Dickinson Biosciences Immunocytometry Systems, San Jose, CA) and the proportion of cells in the G0/G1, G2/M and S phase was estimated using the ModFit cell-cycle analysis program (v3.0, Verity Software House, Topsham, ME). FACS measurements were performed in three independent experiments.

*Note: Supplementary Information is available on the Nature Cell Biology website.*

#### ACKNOWLEDGEMENTS

We thank all the members of our laboratory for helpful discussions. We are also grateful to N. Minato and Y. Hamazaki for help with FACS analysis. This work was supported in part by a Grant-in-Aid for Scientific Research (B) to Sa.T. from the Ministry of Education, Culture, Sports, Science and Technology of Japan.

#### COMPETING FINANCIAL INTERESTS

The authors declare that they have no competing financial interests.

Received 24 January 2005; accepted 21 March 2005

Published online at <http://www.nature.com/naturecellbiology>.

- Lange, B. M. & Gull, K. A molecular marker for centriole maturation in the mammalian cell cycle. *J. Cell Biol.* **130**, 919–927 (1995).
- Nakagawa, Y., Yamane, Y., Okanou, T., Tsukita, Sh. & Tsukita, Sa. Outer dense fiber 2 is a widespread centrosome scaffold component preferentially associated with mother centrioles: its identification from isolated centrosomes. *Mol. Biol. Cell* **12**, 1687–1697 (2001).
- Doxsey, S. Re-evaluating centrosome function. *Nature Rev. Mol. Cell Biol.* **2**, 688–698 (2001).
- Rieder, C. L., Faruki, S. & Khodjakov, A. The centrosome in vertebrates: more than a microtubule-organizing center. *Trends Cell Biol.* **11**, 413–419 (2001).
- Bornens, M. Centrosome composition and microtubule anchoring mechanisms. *Curr. Opin. Cell Biol.* **14**, 25–34 (2002).
- Kochanski, R. S. & Borisy, G. G. Mode of centriole duplication and distribution. *J. Cell Biol.* **110**, 1599–1605 (1990).
- Chretien, D., Buendia, B., Fuller, S. D. & Karsenti, E. Reconstruction of the centrosome cycle from cryoelectron micrographs. *J. Struct. Biol.* **120**, 117–133 (1997).
- Rieder, C. L. & Borisy, G. G. The centrosome cycle in PtK<sub>2</sub> cells: asymmetric distribution and structural changes in the pericentriolar material. *Biol. Cell* **44**, 117–132 (1982).
- Vorobjev, I. A. & Chentsov Yu, S. Centrioles in the cell cycle. I. Epithelial cells. *J. Cell Biol.* **93**, 938–949 (1982).
- Wheatley, D. N. *The Centriole: A Central Enigma of Cell Biology* (Elsevier Biomedical Press, Amsterdam, USA, 1982).
- Paintrand, M., Moudjou, M., Delacroix, H. & Bornens, M. Centrosome organization and centriole architecture: their sensitivity to divalent cations. *J. Struct. Biol.* **108**, 107–128 (1992).
- Mogensen, M. M., Malik, A., Piel, M., Bouckson-Castaing, V. & Bornens, M. Microtubule minus-end anchorage at centrosomal and non-centrosomal sites: the role of ninein. *J. Cell Sci.* **113**, 3013–3023 (2000).
- Chang, P., Giddings, T. H. Jr, Winey, M. & Stearns, T.  $\alpha$ -Tubulin is required for centriole duplication and microtubule organization. *Nature Cell Biol.* **5**, 71–76 (2003).
- Gromley, A. *et al.* A novel human protein of the maternal centriole is required for the final stages of cytokinesis and entry into S phase. *J. Cell Biol.* **161**, 535–545 (2003).
- Ou, Y. Y., Mack, G. J., Zhang, M. & Rattner, J. B. CEP110 and ninein are located in a specific domain of the centrosome associated with centrosome maturation. *J. Cell Sci.* **115**, 1825–1835 (2002).
- Dammermann, A. & Merdes, A. Assembly of centrosomal proteins and microtubule organization depends on PCM-1. *J. Cell Biol.* **159**, 255–266 (2002).
- Sorokin, S. P. Reconstructions of centriole formation and ciliogenesis in mammalian lungs. *J. Cell Sci.* **3**, 207–230 (1968).
- Piperno, G., LeDizet, M. & Chang, X. J. Microtubules containing acetylated  $\alpha$ -tubulin in mammalian cells in culture. *J. Cell Biol.* **104**, 289–302 (1987).
- McGrath, J., Somlo, S., Makova, S., Tian, X. & Brueckner, M. Two populations of node monocilia initiate left-right asymmetry in the mouse. *Cell* **114**, 61–73 (2003).
- Watnick, T. & Germino, G. From cilia to cyst. *Nature Genet.* **34**, 355–356 (2003).
- The European Polycystic Kidney Disease Consortium. The polycystic kidney disease 1 gene encodes a 14 kb transcript and lies within a duplicated region on chromosome 16. *Cell* **77**, 881–894 (1994).
- Mochizuki, T. *et al.* PKD2, a gene for polycystic kidney disease that encodes an integral membrane protein. *Science* **272**, 1339–1342 (1996).
- Pazour, G. J. *et al.* Chlamydomonas IFT88 and its mouse homologue, polycystic kidney disease gene Tg737, are required for assembly of cilia and flagella. *J. Cell Biol.* **151**, 709–718 (2000).
- Hou, X. *et al.* Cystin, a novel cilia-associated protein, is disrupted in the cpk mouse model of polycystic kidney disease. *J. Clin. Invest.* **109**, 533–540 (2002).
- Yoder, B. K., Hou, X. & Guay-Woodford, L. M. The polycystic kidney disease proteins, polycystin-1, polycystin-2, polaris, and cystin, are co-localized in renal cilia. *J. Am. Soc. Nephrol.* **13**, 2508–2516 (2002).
- Praetorius, H. A. & Spring, K. R. Bending the MDCK cell primary cilium increases intracellular calcium. *J. Membr. Biol.* **184**, 71–79 (2001).
- Nauli, S. M. & Zhou, J. Polycystins and mechanosensation in renal and nodal cilia. *Bioessays* **26**, 844–856 (2004).
- Rosenbaum, J. L. & Witman, G. B. Intraflagellar transport. *Nature Rev. Mol. Cell Biol.* **3**, 813–825 (2002).
- Nonaka, S. *et al.* Randomization of left-right asymmetry due to loss of nodal cilia generating leftward flow of extraembryonic fluid in mice lacking KIF3B motor protein. *Cell* **95**, 829–837 (1998).
- Jurczyk, A. *et al.* Pericentrin forms a complex with intraflagellar transport proteins and polycystin-2 and is required for primary cilia assembly. *J. Cell Biol.* **166**, 637–643 (2004).



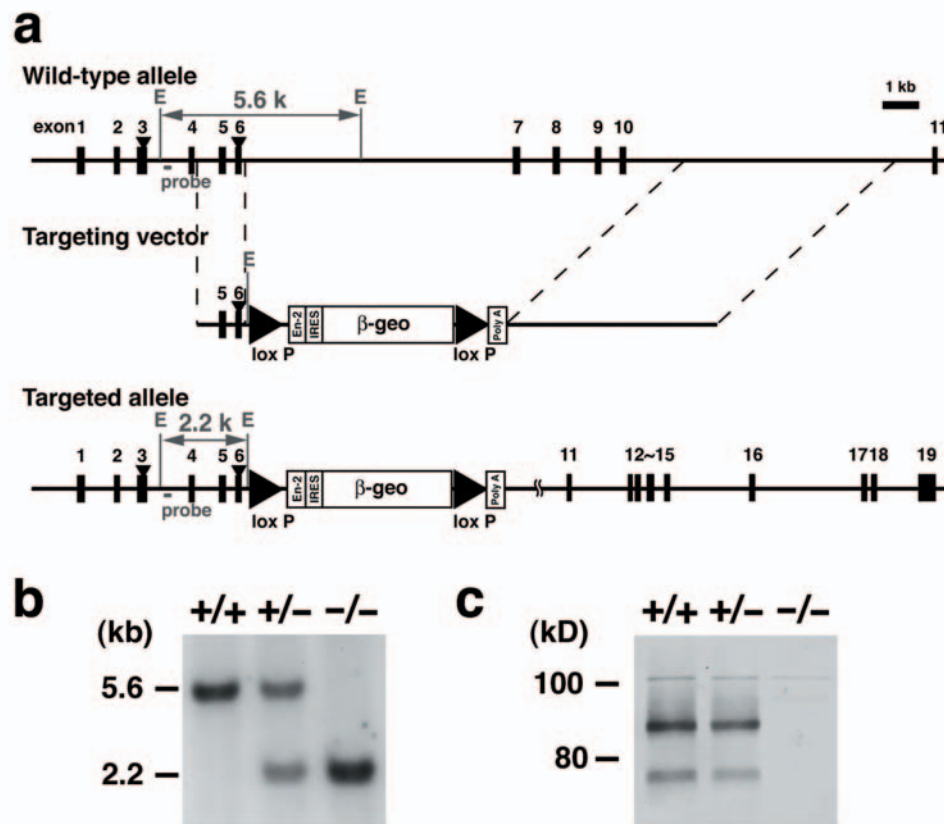


**Figure S1** Generation of *Odf2*-deficient F9 cells. (a) Schematic representation of the wild-type allele, targeting vector and targeted allele of the mouse *Odf2* gene. Depending on the variant species, the first ATG codon was located in exon 3 or 6 (arrowheads). Since exons 7–10 were used in all alternative variants, the targeting vector was designed to replace these exons with  $\beta$ -galactosidase/neomycin-resistance fusion gene ( $\beta$ -geo) combined with engrailed-2 (En-2) which contained splicing acceptor/Internal ribosome entry site (IRES) on its 5'-side and a polyadenylation site (PA) on its 3'-

side, flanked by loxP sites. (b) Genotype analyses by Southern blotting of genomic DNA from wild-type (+/+), heterozygous (+/-) and homozygous (-/-) F9 cells. The *EcoRI* fragments were detected by the 5'probe from wild-type (5.6 kb) and targeted alleles (2.2 kb). (c) Western blotting of wild-type (+/+), heterozygous (+/-) and homozygous (-/-) F9 cells. The whole cell lysates of *Odf2*<sup>+/+</sup>, *Odf2*<sup>+/-</sup>, and *Odf2*<sup>-/-</sup> F9 cells were immunoblotted with anti-*Odf2* pAb. In *Odf2*<sup>+/+</sup> and *Odf2*<sup>+/-</sup> F9 cells, *Odf2* was detected as a ~90-kDa band, whereas *Odf2* was undetectable in *Odf2*<sup>-/-</sup> F9 cells.

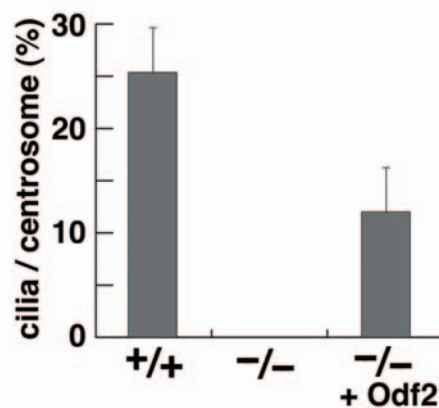


**Figure S2** Quantitative representation of the loss of primary cilia in *Odf2*<sup>-/-</sup> F9 cells. The ratios of primary cilia-carrying cells in total cells were determined by immunofluorescence microscopy with anti-acetylated tubulin mAb. Under the culture conditions used in this study, ~25% of *Odf2*<sup>+/+</sup> cells carried

primary cilia, but all the *Odf2*<sup>-/-</sup> cells lacked primary cilia. When Odf2 was exogenously expressed in *Odf2*<sup>-/-</sup> F9 cells in approximately half the amount of endogenous Odf2 of *Odf2*<sup>+/+</sup> cells (-/-+Odf2), ~12% of these cells appeared to bear primary cilia.